Numerical Simulation of the Thermal Performance of a Dry Storage Cask for Spent Nuclear Fuel

Chi-Ming Lai, University Distinguished Professor
Department of Civil Engineering, National Cheng Kung University
1, University Rd., Tainan City, 701, Taiwan R. O. C.

Rong-Horng Chen, University Distinguished Professor
Department of Mechanical and Energy Engineering, National Chiayi University
300, Syuefu Rd., Chiayi City, 600, Taiwan R. O. C.

Chu-Tsen Liao, Assistant Professor
Department of Creative Design and Architecture, National Kaohsiung University
700, Kaohsiung University Rd., Kaohsiung City, 811, Taiwan R. O. C.

Ting-Yi Wang, Undergraduate Student
Department of Civil and Environmental Engineering, National Kaohsiung University
700, Kaohsiung University Rd., Kaohsiung City, 811, Taiwan R. O. C.

Heui-Yung Chang, Associate Professor
Department of Civil and Environmental Engineering, National Kaohsiung University
700, Kaohsiung University Rd., Kaohsiung City, 811, Taiwan R. O. C.

Keywords: dry storage cask; spent nuclear fuel; salt particle collection; thermal performance; heat transfer

Abstract

In this study, the heat flow characteristics of a dry storage cask were investigated and the effect of installing a salt particle collection device on the thermal performance of the dry storage cask was evaluated, via thermal flow experiments and a computational fluid dynamics (CFD) simulation. The results indicate that there are many inner circulations in the cask's flow channel (the channel width is 10 cm). They affect the channel airflow efficiency, which in turn affects the heat dissipation of the dry storage cask. The daily operating temperatures of the top concrete lid and the upper locations of the concrete cask are higher than permitted by the design specification. The installation of the salt particle collection device has no negative impact on the thermal dissipation performance of the dry storage cask.

1. INTRODUCTION

Taiwan's first and second nuclear power plants use boiling water reactors (BWRs) made by General Electric Corporation (United States). In accordance with the practices abroad, the Taiwan Power Company (Taipower) built dry storage facilities at its nuclear power plants. After using the nuclear fuel for many years, Taipower removed the spent fuel from the reactor core, cooled it in pools, and then stored the spent fuel in dry storage facilities to ensure that the plants had sufficient space in which to operate. At present, the dry storage facility at nuclear power plant No. 1 has been tested. The safety review of the dry storage facilities of nuclear power plant No. 2 has also been completed.

There are few studies regarding the heat transfer performance of dry spent fuel storage casks. Heng et al. (2002) numerically investigated natural convection heat transfer in a horizontally placed dry spent-fuel storage cask. Pugliese et al. (2010) evaluated the integrity of a spent fuel cask under both normal and accident scenario transport conditions, such as impact and rigorous fire events, according to the International Atomic Energy Agency (IAEA) accident test requirements. Koga and Tominaga (2008) investigated the characteristic cooling flow in the annular gap of a concrete cask used to store spent nuclear fuel via a simplified test model. Li and Liu (2016) studied the thermal performance of a vertical dry storage cask with a welded canister containing high-burnup fuel. Kim et al. (2014) investigated heat transfer in a concrete cask such as the one used at the intermediate storage facilities for BWR spent fuel.

Thermal modeling of the temperature profiles of dry casks has been identified as a high-priority item in a U.S. Department of Energy gap analysis. In this work, a two-dimensional thermal model of a vertical dry cask has been established via a computational fluid dynamics (CFD) simulation.

2. RESEARCH METHODS

2.1 Dry storage cask

Dry storage casks are used to store spent nuclear fuel from nuclear power plants. Such casks primarily consist of a nuclear waste steel canister, a concrete cask and a transfer cask. In this paper, the investigated model is based on the dry storage cask that will be employed in Taipower's nuclear power plant No. 2. The layout of the cask is shown in Fig. 1; it is similar to the storage system in NAC's MAGNASTOR-87. One difference is the concrete cask's thickness, which is altered to accommodate the radiation dose limit of the field boundary. Another difference is that an anti-topple lug is installed to facilitate transportation of the concrete cask in the plant (Taiwan Power Company, 2011).

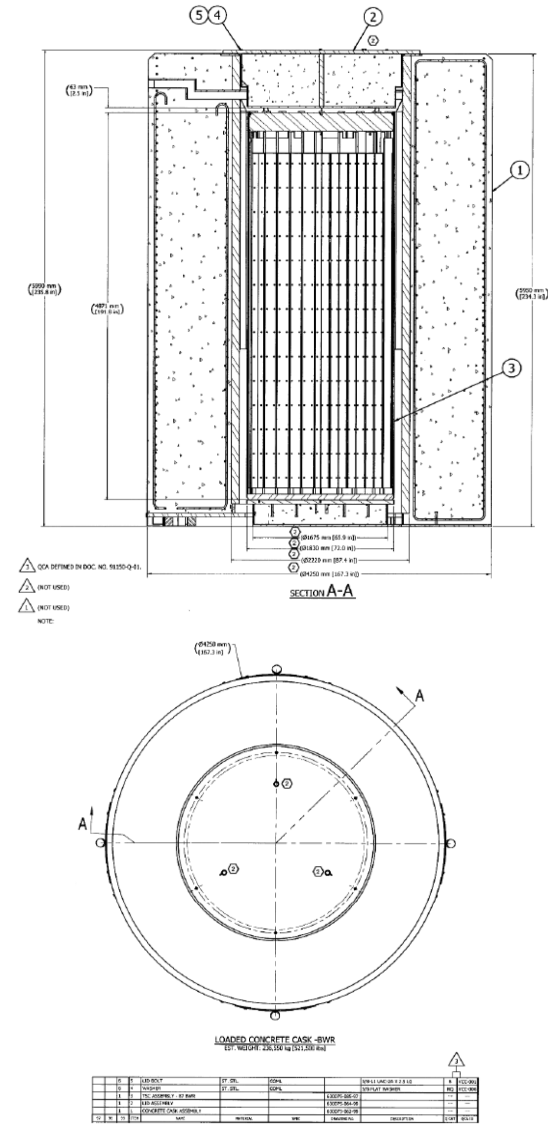

Fig. 1 Design diagram of dry storage cask

Taipower's No. 2 nuclear power plant will store the spent nuclear fuel from the complete GE8x8-2 and ANF8x8-2 rods. The maximum initial average enrichment concentration of U-235 is 3.25% by weight. The maximum average fuel consumption is 35,000 MWD/MTU. The minimum cooling time is 20 years. The maximum decay heat of each fuel bundle is conservatively estimated to be 0.168 kW. Each steel canister can load 87 bundles of nuclear fuel, so the maximum design thermal load of each steel canister is 14.6 kW (1.15 kW/m^3).

For the specified parameters of the BWR fuel stored in the MAGNASTOR system, the maximum initial average enrichment concentration is 3.8% by weight. The maximum average fuel consumption is 60,000 MWD/MTU. The minimum cooling time is 4 years. The maximum decay heat of each bundle is 0.379 kW. The maximum designed thermal load of the sealed steel cylinder is up to 33.0 kW (2.6 kW/m^3) when 87 groups of fuel bundles are stored. Therefore, in this study, a thermal load of 1.15 to 2.6 kW/m^3 for each steel canister is employed in the CFD simulation.

2.2 The investigated model

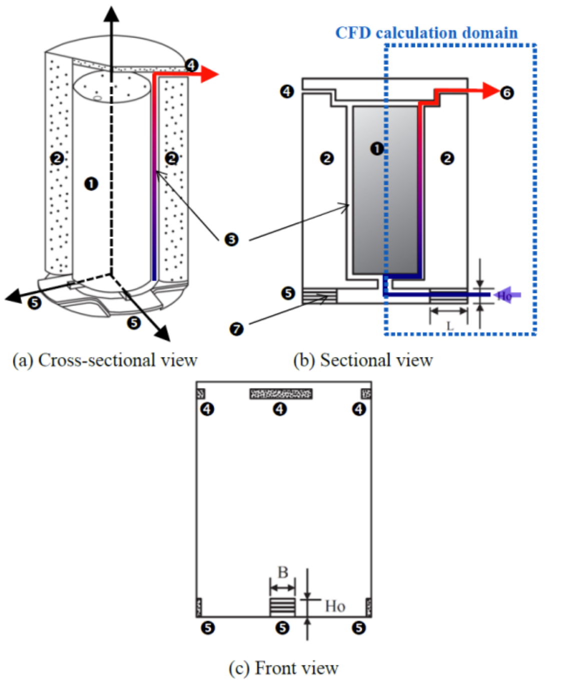

Fig. 2 Schematic diagram of the investigated model (dry storage cask)

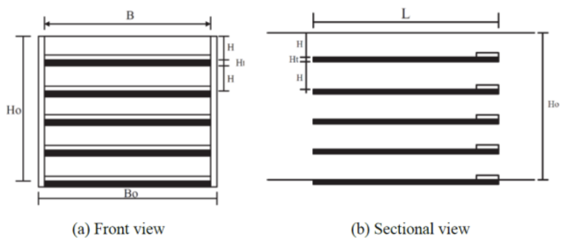

Fig. 3 Schematic diagram of the investigated SPCD

Fig. 2(a) shows the object of this study. It is simplified from Fig 1. Inside the cask, there is a nuclear waste canister containing spent nuclear fuel (symbol❶). Its diameter is 1.8 m, and its height is 5 m. The concrete cask surrounding the steel canister has a thickness of approximately 1 m (❷). A flow channel (❸) of width 10 cm is located between the nuclear waste canister and concrete cask. The decay heat of the nuclear fuel heats the air in the channel. The heated air rises to the channel exit because of the buoyancy effect (❹) and exits from the dry storage cask. The external air enters the channel from the bottom (❺), thus forming a natural ventilation path (❻). In addition to the thermal buoyancy ventilation, the ventilation of the dry storage cask caused by external wind is also taken into account. It should be noted that when the two natural ventilation airflows (airflow induced by buoyancy and wind) merge and conflict, the thermal dissipation performance of the dry storage cask will be compromised. This study does not discuss this topic. It will be addressed in follow-up studies.

In this study, a salt particle collection device (SPCD, ❼) was installed at the inlet (❺), as shown in Fig. 3. The effect of this device on the heat dissipation performance of the dry storage cask was observed. The height of the SPCD is 0.3 m (Ho), and the width is 0.3 m (B). The length of the collection plate and the length L of the SPCD are 0.5 and 1.0 m, respectively. The plate number is 15. The salt capture ratio is approximately 40%.

2.3 CFD simulation

The physical problem under consideration was numerically simulated using a finite volume method to solve the governing equations with the aforementioned boundary conditions. The calculation domain is shown in Fig. 2 (b). A commercial CFD code, PHOENICS, was used to simulate the airflow and temperature distributions. The governing equations solved by PHOENICS include the two-dimensional incompressible Navier-Stokes equation and the convection diffusion equation with the laminar model. These equations can be found in the PHOENICS user manual (Spalding, 2012) or any CFD textbook and thus will not be provided here. A general wall function was employed to bridge the steep variable dependent gradients near the solid surface. The iterative calculation was continued until a prescribed relative convergence of 10^{-3} was satisfied for all the field variables in this problem. The accuracy of the numerical simulation depended on the resolution of the computational mesh, and a finer grid produced more accurate solutions. A grid with approximately 195 x 105 cells was used for the numerical simulation in this study. Increasing the cell number increased the solution accuracy at the expense of significantly increasing the computational resources required.

2.4 Key-section full-scale experiment

In this study, a full-scale test cell for key sections (as shown in the red dotted area of Fig. 4(a)) of the dry storage cask was built and the heat flow patterns of the test cell was experimentally observed (as shown in Figs. 4 (b) and (c)). The experimental results were compared with those obtained from the CFD simulation. The heating power of the spent nuclear fuel in the nuclear waste canister was set to be 400 W/m^2. The length of the plate in the SPCD was 0.5 m.

(1) Hot wall with heating flux

The hot wall (shown in Fig. 4 (b)) is formed by attaching a mica-type heater to a copper plate to simulate the heat generation of spent nuclear fuel. The output power of the heating plate is 400 W/m^2. The thickness of the copper plate is 1 cm. Its function is to ensure that the heating wall is uniformly heated. To control the output power, a power supply is connected to a power meter (TES WM-01) and the heating plate.

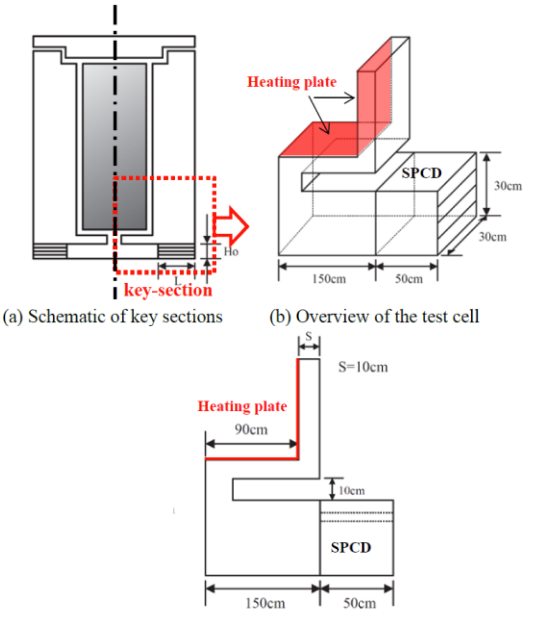

(a) Schematic of key sections (b) Overview of the test cell

(c) Front view of the test cell

Fig. 4 Full-scale experimental model (not to scale)

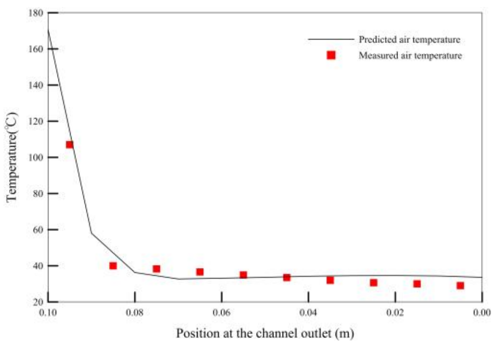

Fig. 5 Comparison of simulation results with the measurement

(2) Temperature, heat flow and channel airflow velocity measurements

In this study, type K thermocouples were used to measure the temperature at multiple locations. The temperatures measured were the surface temperature of the heating plate, the air temperatures at the inlet and outlet of the channels (10 measuring locations each at the inlet and outlet), and the channel wall temperature of the concrete cask. A heat flow meter was placed between the heating plate and the copper plate to measure the heating power. Micro-anemometers were placed at both the entrance (10 locations) and the exit (5 locations) of the flow channel.

(3) Measurement apparatus

The device and data acquisition system included Data Acquisition Units (YOKOGAWA MX-100), a personal computer (PC), heat flux sensors (EKO Instruments MF-180), anemometers (KANOMAX Model 1560) and AC/DC power supply units (Gwinstek APS-1102).

Fig. 5 shows that there was no significant difference between the CFD results and experiment; thus, the reliability of the simulation results was confirmed.

3. RESULTS AND DISCUSSION

In this study, the controlling factors included whether the SPCD was used, the length of the SPCD plate (50 or 100 cm), the heating power of the sealed steel canister (1.15 and 2.6 kW/m^3), and the ambient temperature (25, 30, and 35°C). Based on the design specifications of Taipower (2011), the evaluation criteria were defined as follows: The maximum acceptable temperature for the fuel steel basket was 570°C (abnormal and accidental conditions). The acceptable temperatures for the concrete was either 93.3°C (the average temperature under normal conditions), 148.8°C (the maximum local temperature under normal conditions), or 176.6°C (the maximum local temperature under abnormal or accidental conditions).

3.1 Flow and thermal characteristics of the design configuration

(1) Flow pattern observation

In this section, the flow and thermal characteristics of the dry storage cask were discussed under the following conditions: a 50-cm SPCD is used, the heat dissipation rate of the sealed steel canister is 2.6 kW/m^3, and the ambient temperature is 30°C. Fig. 6 (a) shows the flow velocity distribution. Figs. 6(b)-(c) show the flow pattern. It can be observed from these figures that after the external cold air flows into the dry storage cask from the bottom, the flow separates at the flow's turning locations ①-③. There exist multiple inner circulations in the channel. This affects the heat transferred by the channel airflow from the nuclear waste canister, which in turn affects the temperature distribution in the dry storage cask and leads to a thermal stress problem. On the other hand, owing to the Coanda effect, the high-temperature airflow existing in the dry storage cask merges with the high-temperature airflow from the symmetrical ends at the upper-middle section of the dry storage cask (shown by the symbol ④). The high temperature airflow enclosing the top concrete lid makes heat dissipation at the lid difficult (denoted by the symbol ⑤ in Fig. 5(d)). It even affects the temperature of the concrete cask (indicated by the symbol ⑥ in Fig. 6(d)).

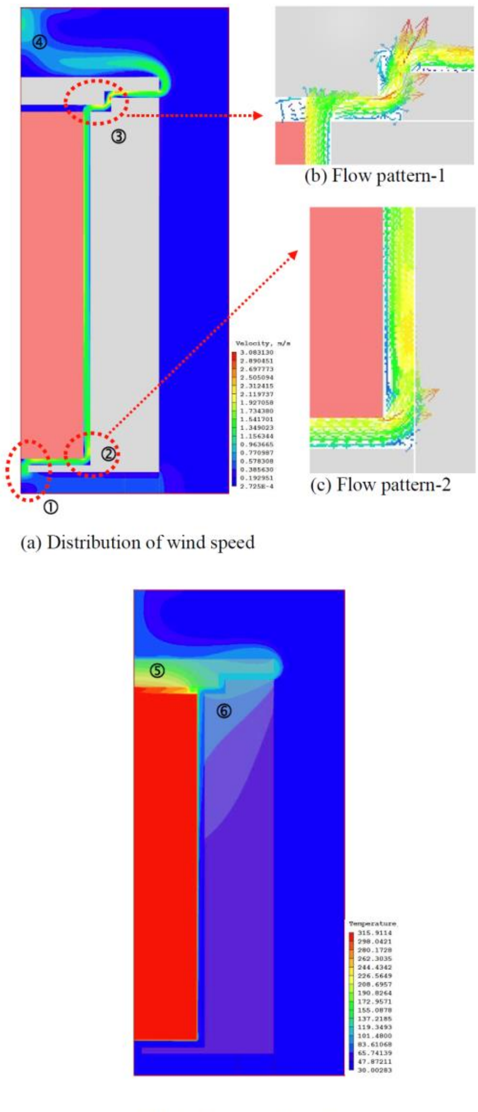

(a) Distribution of wind speed

(b) Flow pattern-1

(c) Flow pattern-2

(d) Distribution of temperature

Fig. 6 Flow and thermal characteristics of the dry storage cask (with the 50-cm-SPCD). (The heat dissipation rate of the sealed steel canister is 2.6 W/m^3. The ambient temperature is 30°C)

(2) Thermal performance

Fig. 7 shows the temperature distribution of the dry storage cask at locations of Y = 3, 2, and 1.5 m.

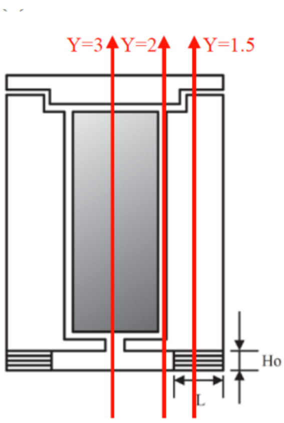

Sectional profiles at different Y locations

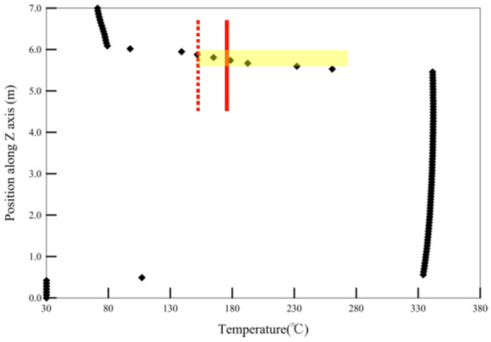

(a) Location Y = 3 m

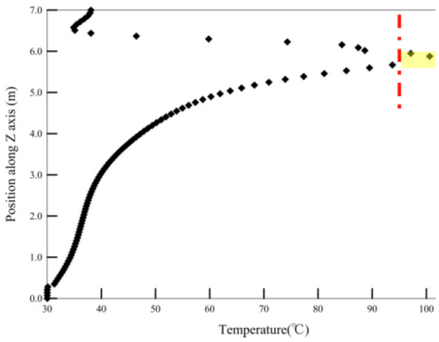

(b) Location Y = 2 m

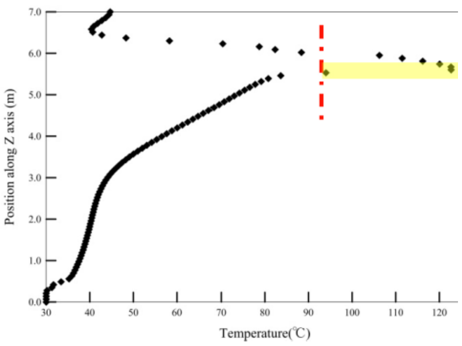

(c) Location Y = 1.5 m

Fig.7 Temperature changes along the height of the dry storage cask (at Y = 3, 2, and 1.5 m) (with the 50-cm SPCD). (The heat dissipation rate of the sealed steel canister is 2.6 kW/m^3. The ambient temperature is 30°C)

This figure shows that the temperature of the nuclear waste canister was approximately 334-342°C, which is less than the evaluation criterion of 570 °C (the maximum acceptable temperature under abnormal or accidental conditions). The temperature of the top concrete lid on the concrete box was as high as 232°C (at height Z = 5.6 m), which is greater than the maximum acceptable temperature (176.6°C, indicated by the red solid line) of concrete under abnormal or accidental conditions. Moreover, the temperatures at the lower and upper halves of the top concrete lid were both greater than the respective maximum acceptable temperatures (176.6°C for the lower half and 148.8°C for the upper half, as indicated by the red dotted line).

Fig. 7 (b) shows that the maximum temperature of the concrete cask was 85.2°C (at height Z = 5.53 m), which satisfies the design requirements. The temperature of the top concrete lid was greater than the acceptable average temperature of the concrete (93.3°C, indicated by the red chain line). Fig. 7(c) shows that the maximum temperature of the concrete cask was 123°C (at height Z = 5.6 m), which is greater than the acceptable average temperature of 93.3°C under normal conditions. The temperature of the lid was also greater than 93.3°C.

Therefore, as a whole, the daily operating temperatures of the top concrete lid and at high locations on the concrete cask (indicated by the symbol ⑥ in Fig. 6(d)) were greater than permitted by the design specifications. Power plant designers should pay attention to the possible structural damage caused by this overheating. Possible solutions to the thermal stress problem discussed above include the following:

(1) Improve the design of the flow channels. The current ventilation flow is through structural spacing. No formal ventilation is designed. If the existing construction cannot be altered, the authors suggest that guide vanes be installed to smooth the airflow, thus increasing the channel airflow's heat dissipation efficiency.

(2) Increase the RC's strength to enhance its resistance to the thermal stress generated.

(3) Use a thermal dissipation design on the top concrete lid and high locations of the concrete cask. The design may include utilization of additives to improve the RC's heat transfer coefficient and installation of heat pipes, among other measures, to ensure that the heat gained inside the RC is smoothly transferred to the outside.

In addition to the heat dissipation problem associated with a single dry storage cask, if several dry storage casks are placed together or external air affects the overall heat dissipation (such as the conflict created by thermal buoyancy-induced airflow and wind, as mentioned in paragraph 1 of Section 2.2), the risk of structural damage caused by poor heat dissipation will be even greater.

3.2 The impact of the SPCD

Compared to devices without SPCDs, utilizing a 50-cm SPCD can increase the heat transferred by the channel airflow by approximately 7.6%. Utilizing a 100-cm SPCD increases the heat transferred via the channel airflow by approximately 7.1% (in both cases, the heating power of the sealed steel canister ranges from 1.15 to 2.6 kW/m^3). Since the SPCD has a plate-like configuration, when the 50-cm SPCD unit is installed in the dry storage cask, its rectification-like effect (Fig. 2 ❼ and Fig. 3) increases the average rate of the channel airflow (compared with cases without SPCDs). However, when the plate length is increased from 50 to 100 cm, the average flow rate is slightly reduced owing to the increase in the flow friction. Compared to devices without SPCDs, the average flow rate of the dry storage cask with a 100-cm SPCD is greater, and thus, more heat is transferred by the channel airflow.

4. CONCLUSION

In this study, based on a CFD simulation and heat flow experiments, the heat flux characteristics of a dry storage cask were investigated and the effect of an SPCD on the heat dissipation performance of the dry storage cask was evaluated. The object studied was a dry storage cask with nuclear waste canisters (with a diameter of 1.8 m and a height of 5 m) containing spent nuclear fuel and a surrounding 1-m-thick concrete cask. The flow channel between the nuclear waste canister and concrete casks has a spacing of approximately 10 cm. The results indicated that there are multiple inner circulations in the airflow channel. This affects the heat transferred by the channel airflow from the nuclear waste canister, which in turn affects the temperature distribution of the dry storage cask and results in thermal stress. Overall, the daily operating temperatures in the top concrete cover lid and the upper locations of the concrete cask were greater than permitted by the design specification. Power plant designers should pay attention to the possible structural damage caused by this overheating. The SPCD does not adversely affect the heat dissipation performance of the dry storage cask.

ACKNOWLEDGEMENT

The authors gratefully acknowledge the financial support from the Ministry of Science and Technology, R.O.C. under Grant No. 106-NU-E-390-001-NU. The authors also thank the Fuel Cycle and Materials Administration, Atomic Energy Council, R.O.C. for providing their insight and expertise that greatly assisted the research.

REFERENCE

Kim H.M., No H.C., Bang K.S., Seo K.S., Lee S.H., Development of scaling laws of heat removal and CFD assessment in concrete cask air path, Nuclear Engineering and Design 278 (2014) 7-16.

Koga T., Tominaga Y., Heat removal characteristics of a concrete cask by a simplified test model, Nuclear Engineering and Design 238 (2008) 1189-1195.

Li J., Liu Y.Y., Thermal modeling of a vertical dry storage cask for used nuclear fuel, Nuclear Engineering and Design 301 (2016) 74-88.

Pugliese G., Lo Frano R., Forasassi G., Spent fuel transport cask thermal evaluation under normal and accident conditions, Nuclear Engineering and Design 240 (2010) 1699-1706.

Spalding DB. The PHOENICS Encyclopedia. London: CHAM Ltd.; 2012.

Taiwan Power Company: Analysis Report on the Safety of a Dry Storage System in the No.2 Nuclear Power Plant, December 2011. (in Chinese)

Xie H., Gao Z., Zhou Z., A numerical investigation of natural convection heat transfer in horizontal spent-fuel storage cask, Nuclear Engineering and Design 213 (2002) 59-65.